Archimer
http://archimer.ifremer.fr

Modeling flocculation processes: Intercomparison of a size class-based model and a distribution-based model

Joeran Maerz[a, *], Romaric Verney[b], Kai Wirtz[c] and Ulrike Feudel[a]

[a] Institute for Chemistry and Biology of the Marine Environment, University of Oldenburg, POB 2503, 26111 Oldenburg, Germany
[b] Ifremer, Hydrodynamics and Sediment Dynamics Laboratory (DYNECO/PHYSED), BP 70, 29280 Plouzané, France
[c] Institute for Coastal Research, GKSS Research Center, Geesthacht, Germany

* Corresponding author :J. Maerz, Tel.: +49 441 798 3634; fax: +49 441 798 3404, email address: maerz@icbm.de

Abstract:

Modeling suspended particulate matter (SPM) dynamics is essential to calculate sediment transport budgets and to provide relevant knowledge for the understanding of biogeochemical cycles in coastal waters. Natural flocs are characterized by their size, shape, structure and density that determine their settling velocity and therefore their vertical as well as horizontal transport. During transport, several processes, in particular aggregation and fragmentation, alter these particle properties. In the present study, we compare two different 0D modeling approaches for flocculation processes, a size classbased (SCB) model and a distribution-based (DB) model that follows the first moment of the particle distribution function. The study leads to an improved understanding of both models, which aim to better resolve SPM dynamics in spatial and ecosystem models in the near future. Both models are validated using data from laboratory experiments. The time evolution of the particle dynamics subjected to tidal forcing is represented equally well by both models, in particular in terms of (i) the mean diameter, (ii) the computed mean settling velocity and (iii) the particle size distribution. A sensitivity study revealed low sensitivity to changes in the collision efficiency and initial conditions, but a high sensitivity with respect to the particles' fractal dimension. The latter is an incitation to enhance the knowledge on processes related to changes of fractal dimension in order to further improve SPM transport models. The limitations of both models are discussed. The model intercomparison revealed that the SCB model is useful for studies focussing on the time evolution of floc distributions, especially under highly variable conditions. By contrast, the DB model is more suitable for studies dealing with larger spatial scales and, moreover, with coupled marine physical–biogeochemical systems, as it is computationally very effective.

Keywords: Suspended particulate matter (SPM); Flocculation/aggregation; Size class-based model; Distribution-based model; Tidal dynamics; Model comparison

1 Introduction

Modeling suspended particulate matter (SPM) dynamics is essential to calculate sediment transport budgets. Furthermore, SPM models provide knowledge on turbidity, on the fate of both particulate organic and inorganic matter, and on particle-reactive chemicals that are relevant quantities for modeling and understanding marine ecosystems.

Natural flocs (or similar: aggregates, particles) are composed of clay, silt and particulate organic matter. They can be characterized by their size, shape, structure (fractal dimension) and density. These properties determine the settling velocity and hence the vertical and lateral transport. Flocs in suspension experience various processes like aggregation, fragmentation, repacking, remineralization, deposition, and eventually subsequent resuspension. Hence, their properties can dynamically change with time. Ideally, these changes and their effects on floc settling velocity should be represented in sediment transport models.

So far, sediment transport models mainly consider semi-empirical relationships between settling velocity and environmental variables, e. g. SPM concentration, shear rate or salinity (developed by e. g. Krone, 1962; Van Leussen, 1994; Manning and Dyer, 1999, 2007). These relationships were obtained from field or laboratory measurements. Therefore, they are not necessarily applicable elsewhere.

In order to represent the processes of aggregation and fragmentation more realistically, various models have been developed on the basis of the Smoluchowski equation (von Smoluchowski, 1917) assuming a spatially well-mixed environment (zero-dimensional (0D) model). Most of these models only consider changes in size, whereas a few of them also consider a size dependent changing fractal dimension (Maggi et al., 2007; Son and Hsu, 2008).

* Corresponding author. Address: ICBM – University of Oldenburg, POB 2503, 26111 Oldenburg, Germany, Phone number: ++49-(0)441-798-3634, Fax: ++49-(0)441-798-3404
   Email addresses: `maerz@icbm.de` (Joeran Maerz),
`romaric.verney@ifremer.fr` (Romaric Verney), `wirtz@gkss.de` (Kai Wirtz),
`u.feudel@icbm.de` (Ulrike Feudel).

In general, there are two possibilities to represent the size distribution of particles in models. In *size class-based* (SCB) models the floc distribution is represented in terms of size classes (e. g. McAnally and Mehta, 2002; Maggi et al., 2007; Verney et al., 2010, this issue) or only their central moments (Prat and Ducoste, 2006). Other approaches use a characteristic diameter (Son and Hsu, 2008; Winterwerp, 1998; Winterwerp et al., 2006) while Maerz and Wirtz (2009) use the average floc size of a continuous floc size distribution function leading to *distribution-based* (DB) models.

All of these models can be potentially included in SPM transport models. But only a few applications were achieved in an 1 D vertical model (Krishnappan and Marsalek, 2002; Winterwerp, 2002) and in a 2 D model (Krishnappan, 1991). This might have several reasons, e. g. limitations due to computational costs, increasing model complexity, difficulty of parametrization and the so far little understanding of processes changing aggregates' properties like fractal dimension, size and density. Models using a characteristic diameter or an average radius need less computational time than models that explicitly resolve a number of size classes. For this reason, they might be more appropiate for a coupling to a 3 D transport model. However, DB models use some approximations and thus, it is an open question, how well they reflect the dynamics of the whole floc distribution compared to SCB models. In order to point out assets and drawbacks of the two different modeling approaches the present study focuses on an intercomparison of a SCB and a DB model. Both models are validated with the same data set from a laboratory experiment. This provides a better understanding of both models, which aim to resolve SPM size dynamics in both higher dimensional SPM transport and marine ecosystem models in the near future.

2   Description of the two models

Both 0 D models (SCB and DB) represent the processes of aggregation (using the Smoluchowski equation) and fragmentation due to shear.

The size class-based (SCB) model, developed by Verney et al. (2010, this issue) represents the floc distribution in terms of distinct size classes. By contrast, the distribution-based (DB) model, developed by Maerz and Wirtz (2009), uses an underlying continuous distribution function and only follows the average radius. Therefore it aims for reducing model complexity. In the following, the common features of the two models are described.

Both aggregation models are based on the formulation of von Smoluchowski (1917) that is given by

$$\frac{\mathrm{d}\,n(m)}{\mathrm{d}\,t} = \frac{1}{2} \int\limits_0^m \alpha(m - m', m')\, n(m - m') \cdot n(m')\, I(m - m', m')\, \mathrm{d}m'$$

$$- n(m) \int\limits_0^\infty \alpha(m, m')\, n(m') \cdot I(m, m')\, \mathrm{d}m' \tag{1}$$

where the first term of the right hand side is the gain of particles n of mass m by aggregation of smaller particles $n(m - m')$ and $n(m')$ with the collision efficiency α and the collision frequency I. The second term describes the loss of particles due to aggregation with other particles. For simplification, in both models we assume a size-independent collision efficiency. Furthermore we focus on the aggregation due to turbulent shear $G = (\epsilon/\nu)^{1/2}$ (ϵ being the turbulent energy dissipation rate and ν being the kinematic viscosity of the fluid) using the rectilinear approach for the collision frequency, here written for particles in classes i and j with radii r_i and r_j, respectively

$$I_{G,i,j} = 1.3\, G\, (r_i + r_j)^3 \,. \tag{2}$$

Aggregation due to differential settling is believed to be less relevant compared to shear-induced aggregation (Lick et al., 1993) and Brownian motion is only relevant for particles $< 1\,\mu$m (McCave, 1984). We hence neglect these processes of aggregation. In order to simulate the fragmentation of particles, a simplified fragmentation kernel (with f_B being a fragmentation factor) is used for a particle of diameter D_i:

$$B_{G,i} = f_\mathrm{B}\, G^{1.5}\, D_i^2 \,, \tag{3}$$

that is close to the formulation proposed by Winterwerp (1998). The detailed implementation of both, the aggregation and the fragmentation kernel, in the two flocculation models are described in Section 2.1 and 2.2.

2.1 Size class-based model

The size class-based (SCB) model, developed to reproduce the flocculation and fragmentation processes, is briefly described hereafter, but an extended description can be found in Verney et al. (2010, this issue). The SCB model is based on the population equation system originally proposed by von Smoluchowski (1917) that describes the floc population in N discrete size classes. Here, each of the used N (=15) classes corresponds to a specific particle size (and hence a related mass). They are logarithmically distributed starting from the primary particle diameter $D_\mathrm{p} = 4\,\mu$m to the maximum floc size

$D_{\max} = 1500\,\mu$m by using the following relation:

$$D_i = D_{\mathrm{p}}^{1+\frac{i-1}{N-1}\cdot\left(\frac{\log_{10}(D_{\max})}{\log_{10}(D_{\mathrm{p}})}-1\right)} \tag{4}$$

where D_i is the floc diameter in size class i. In order to reduce the number of size classes required to realistically reproduce flocculation processes, an interpolated aggregation scheme is applied to represent the particle distribution. Each size class represents specific characteristics like floc size and mass. Newly formed flocs that have a mass and size in-between those classes are distributed in the two neighbour classes by using a mass-weighted linear interpolation (Prakash et al., 2003; Xu et al., 2008). Mass conservation is ensured by the conversion of the redistributed mass into the related number of aggregates of the class specific mass by using the below described fractal concept (see Figure 1 and for a more detailed description Verney et al., 2010, this issue). This allows to use a much smaller number of size classes compared to
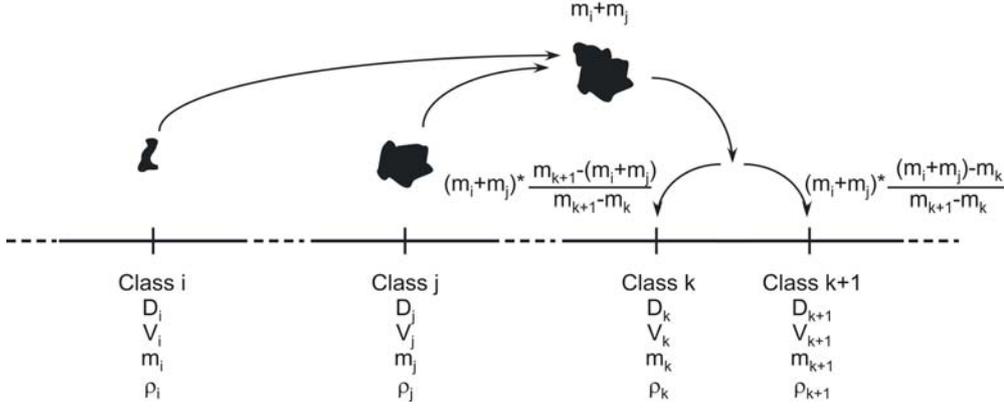

Fig. 1. Aggregation of flocs of mass m_i and m_j into mass $m_i + m_j$ and subsequent distribution into the nearest size classes by using a mass-weighted interpolation. V_i and ρ_i are the volume and the effective density of a floc in size class i, respectively.

the number of potentially newly formed floc sizes, and therefore reduces the computation time. The fractal behaviour of flocs is represented according to the description by Kranenburg (1994). The main characteristic sizes of flocs (with diameter D_i, mass m_i and density $\rho_{\mathrm{f},i}$) can be expressed via the fractal dimension d_f:

$$m_i = \rho_{\mathrm{s}}\frac{\pi}{6}D_{\mathrm{p}}^3\left(\frac{D_i}{D_{\mathrm{p}}}\right)^{d_f} \tag{5}$$

$$\rho_{\mathrm{f},i} = \rho + (\rho_{\mathrm{s}} - \rho)\left(\frac{D_{\mathrm{p}}}{D_i}\right)^{3-d_f} \tag{6}$$

5

where ρ and ρ_s are the density of water and of the primary particles, respectively. Exchanges between classes are allowed through flocculation processes and governed by the kernels for shear aggregation $I_{G,i,j}$ (cf. to Eq. (2)) and fragmentation $B_{G,i}$:

$$\frac{\mathrm{d}\,n_k}{\mathrm{d}\,t} = \alpha\,\frac{1}{2}\sum_{i+j\simeq k} n_i\,n_j\,I_{G,i,j} - \alpha\sum_{i=1}^{N} n_i\,n_k\,I_{G,i,k}$$
$$+ \sum_{i\simeq k+1}^{N} F_{\mathrm{D},i,k}\,B_{G,i}\,n_i - B_{G,k}\,n_k \quad (7)$$

where n_k is the number of particles in class k (in $\#/\mathrm{m}^3$) and $F_{\mathrm{D},i,k}$ the distribution function of fragmented flocs. Note that $i + j \simeq k$ is written instead of the usually used $i + j = k$ to account for the above described mass-conservative interpolation scheme. In the present study, a binary fragmentation is used, i. e. the fragmentation of a particle of mass m_i results in two particles of equal mass $m_i/2$. The fragmentation kernel, Eq. (3), is directly used

$$B_{G,i} = f_{\mathrm{B}}\,G^{1.5}\,D_i^2 \qquad (8)$$

where f_{B} is a constant integrating the cohesiveness of particles. In order to optimize computation time, exchange kernels are calculated once at the initialization with discrete values of G ranging from 0 to a maximum value reproduced experimentally, i. e. $G_{\mathrm{max}} = 12\,\mathrm{s}^{-1}$.

2.2 Distribution-based model

In order to reduce model complexity, Maerz and Wirtz (2009) used the moment closure approach of Wirtz and Eckhardt (1996) to develop a distribution-based (DB) aggregation model. The general idea is to follow only the first moment of the concentration distribution function and the total concentration. The concentration distribution function C_i is given by the SPM mass per volume and bin width ΔR_i in each size class i. Hence, the total concentration is $C = \sum_i C_i\,\Delta R_i$. The average radius of the concentration distribution $\langle r \rangle$ is represented by

$$\langle r \rangle = \sum_i r_i\,\frac{C_i\,\Delta R_i}{C} \qquad (9)$$

6

where r_i is the radius in size class i. The change of $\langle r \rangle$ can therefore be written as

$$\frac{\mathrm{d}\langle r \rangle}{\mathrm{d}\,t} = \sum_i r_i \frac{\dot{C}_i\,\Delta R_i}{C} - \frac{\dot{C}}{C} \sum_i r_i \frac{C_i\,\Delta R_i}{C} \tag{10}$$

where $\dot{C}_i$ and $\dot{C}$ are the changes of the concentration in size class i and in total, respectively. Eq. (10) can also be written as

$$\frac{\mathrm{d}\langle r \rangle}{\mathrm{d}\,t} = \langle r \cdot \hat{\mu} \rangle - \langle r \rangle \cdot \langle \hat{\mu} \rangle \tag{11}$$

where $\hat{\mu}$ is the relative growth rate defined as $\hat{\mu}_i = \dot{C}_i/C_i$. Expanding $\hat{\mu}$ in a Taylor-series around $\langle r \rangle$ and using a moment closure leads to (see Wirtz and Eckhardt, 1996)

$$\frac{\mathrm{d}\langle r \rangle}{\mathrm{d}\,t} \simeq \delta r^2 \cdot \frac{\mathrm{d}\,\hat{\mu}(\langle r \rangle)}{\mathrm{d}\,r} \,. \tag{12}$$

Hence, temporal changes of $\langle r \rangle$ follow a local gradient of $\hat{\mu}$. The rate of change is proportional to the gradient itself and the variance of the aggregate concentration distribution δr^2. This can also be seen, if one writes Eq. (10) as

$$\frac{\mathrm{d}\langle r \rangle}{\mathrm{d}\,t} = \sum_i r_i \cdot (\hat{\mu}_i - \langle \hat{\mu} \rangle) \frac{C_i\,\Delta R_i}{C} \tag{13}$$

where each rate (summand) contributing to the change of $\langle r \rangle$ is dependent on the difference between the relative growth rate $\hat{\mu}_i$ in size class r_i and the average relative growth rate $\langle \hat{\mu} \rangle$ multiplied by the fraction of the concentration corresponding to that size class. So, if the relative growth rate and the size covary, the change of the average radius is high (see also Eq. (11)).

The moment approximation does not require specific assumptions on the underlying distribution function, but looses accuracy for non-Gaussian distributions. The latter is also the reason for using $\langle r \rangle$ as state variable because the concentration distribution is closer to a Gaussian distribution than the number distribution of the aggregates.

In the following, we use Eq. (12) to develop the aggregation formulation for a continuous distribution function. In a first step, we substitute the mass by the radius in Eq. (1). It is important to note that at this step, mass conservation is not fulfilled any more, but will be assured afterwards. The resulting equation can be transformed in order to describe the change of the concentration for each radius by multiplying with the weight of an aggregate $w(r) = w_0 \cdot r^{d_f}$.

The weight factor w_0 is written as $w_0 = 2^{d_f}\,\rho_{\mathrm{s}}\,\pi\,D_{\mathrm{p}}^{3-d_f}/6$. Division of this transformed equation by the concentration $C(r)$ results in the relative growth rate $\hat{\mu}(r)$. As underlying aggregate number distribution $n(r)$, an exponential approach is used in $\hat{\mu}$,

$$n(r) = N_0 \cdot \exp(-\beta r) \tag{14}$$

where the factor β and N_0 denote the slope and the intersection with the ordinate, respectively, for the straight line in a logarithmic representation. The assumption of an exponential number distribution can be justified by measurements for aggregate distributions in tidal areas (Lunau et al., 2006). Now, we use the rectilinear kernel for shear, Eq. (2), in $\hat{\mu}$ and solve the integrals in $\hat{\mu}$.

To assure mass conservation, we have to require that the total concentration does not change, resulting in the condition $\langle \hat{\mu} \rangle = 0$. The average of the relative growth rate can be calculated by using a second order closure

$$\langle \hat{\mu} \rangle = \hat{\mu} + y \cdot \frac{\partial^2\,\hat{\mu}}{\partial\,r^2} = 0 \tag{15}$$

as correction with choosing y in such a way that Eq. (15) is fulfilled. The coefficient y depends on the distribution function and would be given by $y = 0.5\,\delta r^2$ for a Gaussian distribution. Using the integral of the concentration distribution

$$C = \int\limits_0^\infty C(r)\,\mathrm{d}r = \int\limits_0^\infty n(r)\,w(r)\,\mathrm{d}r = \int\limits_0^\infty N_0\,\exp(-\beta r)\,w_0\,r^{d_f}\,\mathrm{d}r \tag{16}$$

as well as the resultant relations $\delta r^2 = \langle r \rangle^2/(d_f+1)$, $\beta = (d_f+1)/\langle r \rangle$ together with $\langle \hat{\mu} \rangle$ in Eq. (12) leads to

$$\frac{\mathrm{d}\,\langle r \rangle}{\mathrm{d}\,t} = \alpha\,G\,K_G(d_f)\,\frac{C}{w_0}\,\langle r \rangle^{4-d_f} \tag{17}$$

where $K_G(d_f)$ is a function of the fractal dimension d_f and describes the correction for the difference between the underlying concentration distribution and a Gaussian distribution. $K_G(d_f)$ is given by

$$K_G(d_f) = 0.65\,\frac{(d_f + 1)^{d_f-1}(2\,d_f^4 + 3\,d_f^3 - 3\,d_f^2 + 17\,d_f + 57)}{(d_f^2 + d_f - 1)\,\Gamma(d_f + 2)} \tag{18}$$

where $\Gamma(x)$ is the Gamma function.

For the change of the $\langle r \rangle$ due to fragmentation, the fragmentation kernel (Eq. (3)) is used for the mean radius by multiplying it with $2\langle r \rangle$

$$\frac{\mathrm{d}\langle r \rangle}{\mathrm{d}t} = -8\, f_{\mathrm{B}}\, G^{1.5}\, \langle r \rangle^3 \tag{19}$$

resulting in a similar formulation as proposed in Winterwerp (1998) who considered a characteristic diameter of a particle distribution.

3 Results

In order to evaluate the performances of DB and SCB modeling approaches, model results are compared with experimental data reproducing the behaviour of a floc population during a tidal cycle. A comparison is made i) in terms of the mean floc diameter weighted by the projected area of a floc and ii) by their distribution. Furthermore, as the vertical flux of sediment is of main interest in higher dimensional models, we calculate an average settling velocity depending on the calculated distribution. Next, the sensitivity of both models with respect to several key parameters such as the fractal dimension or the initial distribution is examined (see Section 3.3).

3.1 Validation data

For validation of both models an experimental data set is used (Verney et al., 2010, this issue). In this experiment, the floc population was investigated under changing hydrodynamic conditions. Turbulent shear was changed stepwise between $G = 0$ and $12\,\mathrm{s}^{-1}$ to mimic a tidal cycle. That range of turbulent shear was observed during field measurements above intertidal mudflats (Verney et al., 2006). The device consists in a cylindrical test chamber (13 cm width and 20 cm height) equipped with a ten-speed impeller for controlling turbulent agitation. Turbulent kinetic energy inside the chamber was measured by a Doppler velocimeter revealing a fair shear rate homogeneity that makes the experiment suitable for 0 D model comparisons (Mikes et al., 2004; Verney et al., 2009).

Floc sizes were evaluated in terms of the equivalent circular diameter (ECD) and determined by a postprocessing of images derived from a Sony CCD camera system with a pixel resolution of $8\,\mu\mathrm{m}$. The latter limits the consistency of measurements for small flocs. For this reason, particles smaller than $50\,\mu\mathrm{m}$ were not taken into account during the analysis. The concentration distribution is calculated on the basis of the ECD and the related mass using fractal

9

theory, Eq. (5). As inoculum, SPM collected in the upper part of the Seine estuary, France (freshwater part, muddy sediments with a organic matter content of around $5\,\%$) in winter 2005, was used in a concentration of $93\,\mathrm{mg} \cdot \mathrm{L}^{-1}$. After filling the test chamber, high turbulence mixing was applied to reach a microfloc population as initial condition. An upstream flow in the middle of the test chamber prevented potential deposition of particles at the bottom during times of shear.

During the first two hours of constant turbulent shear $G = 1\,\mathrm{s}^{-1}$, the mean ECD increases up to ca. $250\,\mu\mathrm{m}$. During a stepwise increase of shear up to $G = 12\,\mathrm{s}^{-1}$, the mean ECD decreases down to ca. $60\,\mu\mathrm{m}$. After this time, a decrease of the shear rate leads again to an increasing mean ECD that decreases during time spans of no shear due to settling of the particles followed by a second cycle of changing shear rates (see Figure 2).

3.2 Model and data comparison

For model intercomparison and validation, the main parameters used in the SCB and the DB model (initial mean floc size, concentration C, density of primary particles ρ_s) were determined from the laboratory experiment. The primary particle size D_p was set to $4\,\mu\mathrm{m}$ in accordance with other cohesive sediment studies (e. g. Winterwerp, 1998) and the fractal dimension to $d_f = 1.9$ according to estimations made during similar laboratory experiments of Verney et al. (2009). Therefore, both models use identical parameter values (cf. Table 1) except for the break-up factor f_B and the collision efficiency α that are varied independently for both models in order to minimize the error between model results and data. The error is calculated from the least square method on the entire dataset excluding the period, where settling is the dominant process for size distribution changes ($6\,\mathrm{h} < t \leq 7\,\mathrm{h}$) as this process is not taken into account in the model formulation.

3.2.1 Average diameter

As can be seen in Figure 2, both models are in good agreement with the data and follow the size dynamics equally well. We emphasize here again, that the goodness of the data is limited by the lower resolution of the camera system that could lead to an overestimation of the mean diameter of the particles. During time spans where aggregation rates dominate fragmentation rates, the mean floc size increases smoothly. Otherwise, when fragmentation dominates, the mean floc size decreases abruptly and reaches rapidly a new equilibrium related to increasing shear. These two different behaviours are well reproduced by both the SCB and the DB model. They correspond to differences in pro-

Table 1
Parameter set for the reference runs. In case of the break-up factor f_B and the collision efficiency α values are given as DB/SCB values.

Parameter	Description	Value	literature value	Unit
α	collision efficiency	0.18 / 0.4	0.005-0.8 [a]	–
C	Total SPM concentration	0.093	0.01-6 [b]	$kg \cdot m^{-3}$
d_f	fractal dimension	1.9	$1.5 - 2.4$ [c]	–
D_p	diameter of primary particles	$4 \cdot 10^{-6}$	$1 - 10 \cdot 10^{-6}$ [d]	m
f_B	break-up factor	12068 / 48000	– [e]	$s^{0.5} \cdot m^2$
ρ_s	density of primary particles	2600	2300-2800 [f]	$kg \cdot m^3$
μ	dynamic viscosity	$1.02 \cdot 10^{-3}$	$1 - 1.8 \cdot 10^{-3}$	$kg \cdot m^{-1} \cdot s^{-1}$

[a] Kiørboe et al. (1990); Dam and Drapeau (1995) for algae; [b] Guezennec et al. (1999); Manning et al. (2006); [c] Manning and Dyer (1999); [d,f] Fettweis (2008); [e] no measurements available

cess timescales between aggregation (slow response) and fragmentation (fast response): aggregation is caused by the collision of flocs and only a fraction of these collisions leads to aggregation while fragmentation is only a function of floc size, cohesiveness and shear stress. This leads to a steep negative slope, when fragmentation dominates and a more gentle positive slope, when aggregation dominates.

3.2.2 Comparison of the distributions

While the mean floc size reveals the general behavioural trend of the floc population, the analysis of the floc size distribution allows for precisely investigating the changes within the population itself. This examination requires a discretization of the continuous distribution function of the DB model based on the SCB model size class discretization. The interpolation method used in the SCB model for a normalized floc mass distribution C'_i is applied:

$$C'_i = \frac{w_i}{C} \cdot \left(\int_{r_{i-1}}^{r_i} n(r) \frac{w(r) - w_{i-1}}{w_i - w_{i-1}} \, dr + \int_{r_i}^{r_{i+1}} n(r) \frac{w_{i+1} - w(r)}{w_{i+1} - w_i} \, dr \right) \qquad (20)$$

where w_i is the weight of an aggregate of size r_i in the SCB model.

The comparison of the distributions reveals that both models simulate smoother distributions than the ones observed in the laboratory experiment (cf. Figure 3 and 4). Slight discrepancies between the two models can be explained by the
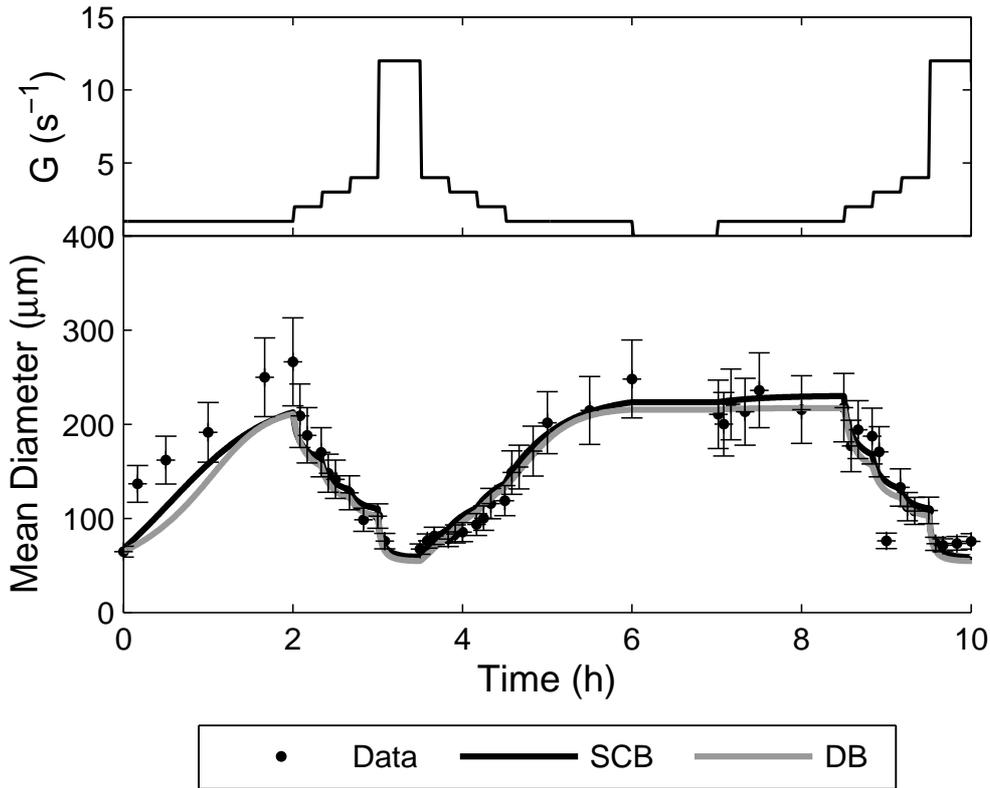
11

Fig. 2. Mean floc size variation during a simulated tidal cycle: comparison between laboratory measurements and models results. Note that the mean diameter of the observed flocs might be overestimated due to limitations of the camera system. SCB: size class-based and DB: distribution-based model.

structure of each model and their underlying assumptions: the SCB model is only controlled by the exchange processes between flocs of each size class while the DB model prescribes the distribution function to represent the floc population. The experimental data suggest that the concentration distribution changes with time and tends to have a peak-like form especially in case of high shear rates. In both models, this behaviour is not properly represented.

3.2.3 Average settling velocity

Different distributions of aggregates have an impact on the vertical fluxes of sediment as macroflocs settle faster than microflocs. This is particularly important for simulating SPM dynamics in spatially explicit models. Therefore, we calculate a theoretical average settling velocity for the experimentally observed particle distribution as well as for both models. The settling velocity v_s of fractal particles with diameter D (e.g. Winterwerp, 1998, without the
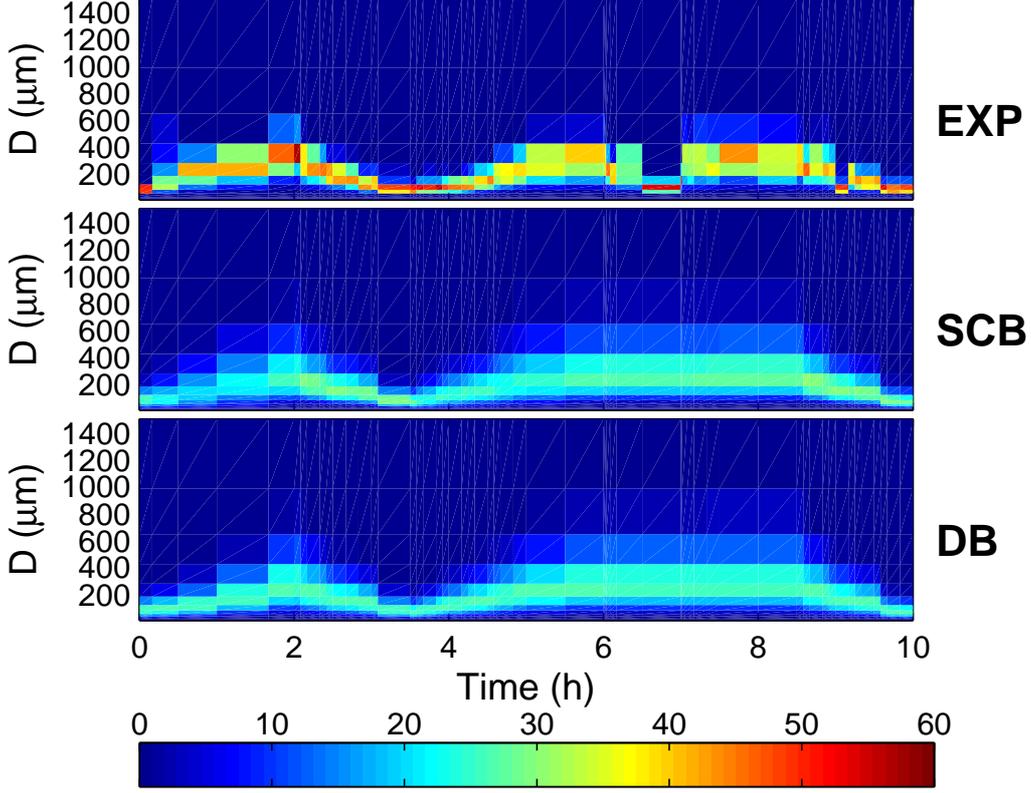
Fig. 3. Normalized concentration in % of the experimentally derived distribution (EXP), size class-based model (SCB) and distribution-based model (DB). Note that both models fail for the time $6\,\mathrm{h} < t \leq 7\,\mathrm{h}$ as settling is not taken into account in the model comparison.

proposed correction term) is given by

$$v_{\mathrm{s}}(D) = \frac{1}{18\,\mu}\,(\rho_{\mathrm{s}} - \rho)\,g\,D_{\mathrm{p}}^{3-d_f}\,D^{d_f-1} \tag{21}$$

where μ is the dynamic viscosity and g is the gravitational acceleration constant. In case of the DB model the average settling velocity can also be computed from the underlying distribution by dividing the total flux (calculated using Eq. (16) and (21)) by the total concentration resulting in

$$\langle v_s \rangle = \frac{1}{18\,\mu}\,(\rho_{\mathrm{s}} - \rho)\,g\,D_{\mathrm{p}}^{3-d_f}\,2^{d_f-1}\,\langle r \rangle^{d_f-1}\left[\frac{4^{d_f}\,(d_f+1)^{1-d_f}\,\Gamma(d_f+0.5)}{2\,d_f\,\sqrt{\pi}}\right] \tag{22}$$

where $\Gamma(x)$ is the Gamma function. Obviously, comparing Eq. (21) and (22), a factor, dependent on d_f, appears when calculating the average settling velocity upon the basis of $\langle r \rangle$. This factor is close to 1 for the value of the fractal
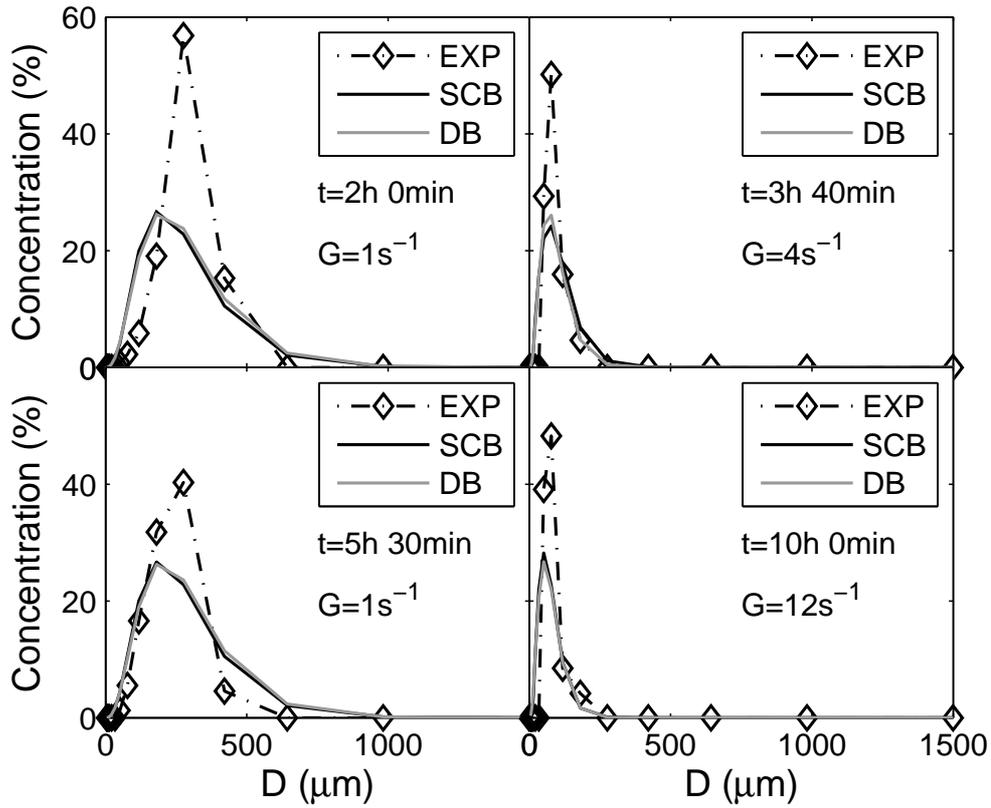
13

Fig. 4. Normalized concentration in % of the experimentally derived distribution (EXP), size class-based (SCB) and distribution-based (DB) model for different times (t).

dimension used in the model comparison. Nevertheless, it is important to emphasize here, that the average settling velocity is not necessarily equal to the settling velocity of a particle of size $\langle r \rangle$ especially if particles tend to be compact.

As can be seen in Figure 5 both models are able to represent the mean settling velocity well after some transient time. Note, that the mean settling velocity calculated from the observed particle distribution might be overestimated due to limitations of the camera system.

3.3 Sensitivity analysis

Some parameters are still inaccessible (like e. g. collision efficiency) or difficult to determine (e. g. fractal dimension) when observing SPM dynamics. It is hence useful to perform a sensitivity study for such parameters in order to estimate the resulting uncertainty in model outcomes. Here, we focus on the
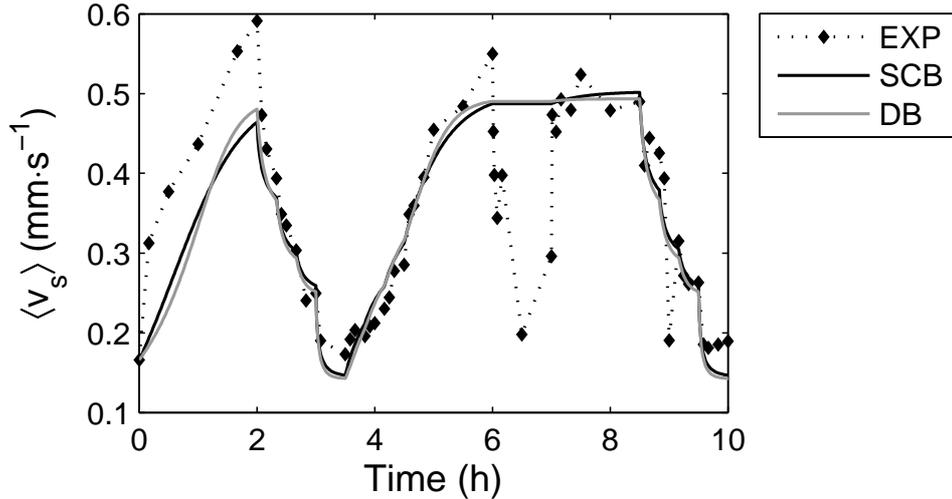
Fig. 5. Mean settling velocity for experimentally observed particles, size class-based model (SCB) and distribution-based model (DB) calculated by Eqs. (21) (data, SCB model) and (22) (DB model). Note, that both models fail for the time $6\,\mathrm{h} < t \leq 7\,\mathrm{h}$ as the models do not account for changes in the size distribution by settling.

fractal dimension d_f, the collision efficiency α and the often unknown or only roughly known initial conditions. Furthermore, since the models differ in their representation of the particle distribution, we study the process of aggregation in more detail.

3.3.1 Initial phase without break-up

When looking only at the process of aggregation without using the fragmentation term, the results of both models show a divergence in the average diameter after a short time. This is enhanced by different values of the collision efficiency α used in both models for the reference runs. But there is another effect that also causes the divergence which is explained in the following. The shape of the distribution function changes in case of the SCB model. This leads to a drastically changed distribution within a short period of time (cf. Figure 6) with an increasing number of large aggregates. As a consequence, the collision frequency increases with time (cf. Eq. (2)) resulting in an increasing relative growth rate for larger size classes that enhances the growth rate of the mean diameter compared to the initial distribution. By contrast, in the DB model the growth rate of $\langle r \rangle$ always relies, due to the model structure, on the prescribed exponential number distribution function. As a consequence, the distribution that would evolve from pure aggregation cannot evolve and is always "forced back" to a prescribed distribution. This model structure dependent mechanism acts as a distribution-internal mass redistribution, and thus, as fragmentation. This additional fragmentation, which is only present in the DB model and not in the SCB model, would result in different vertical

15

fluxes due to discrepancies in the concentration distribution. For this reason, a smaller value of the fragmentation factor f_B has to be chosen for the DB model to compensate the model-dependent artificial fragmentation.
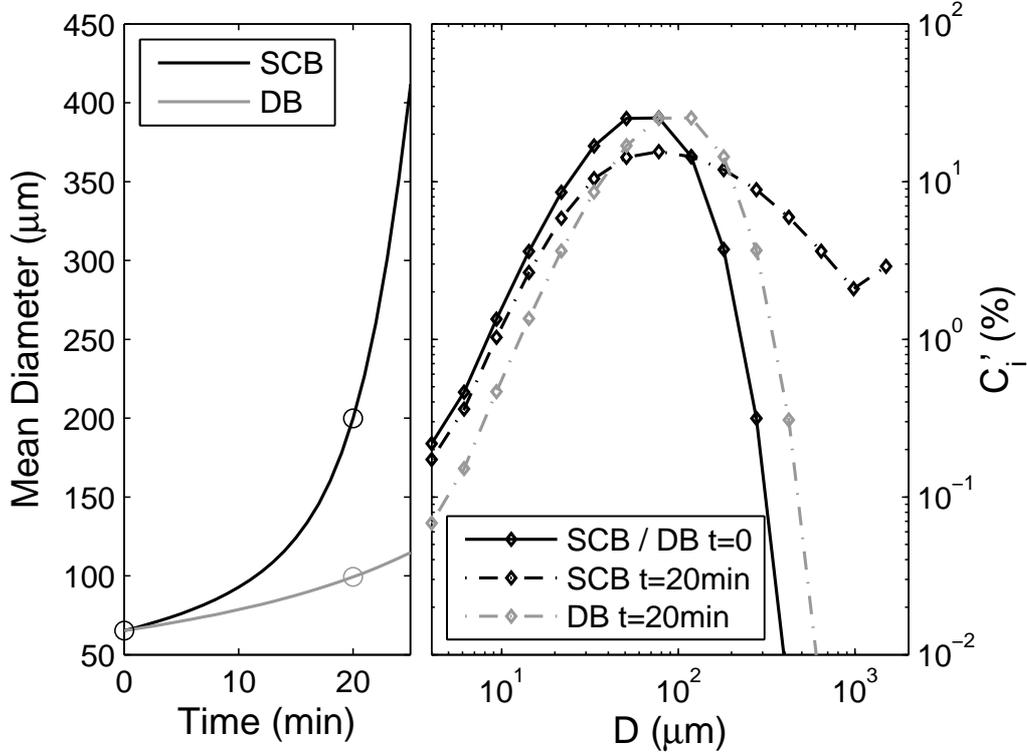

Fig. 6. Left: Time evolution of the mean floc diameter as simulated by the distribution-based (DB) and the size-class based (SCB) model. Right: Floc size distribution computed by both models at simulation start and after 20 min (indicated by open circles in the left panel). Notice that only the term of aggregation is taken into account with the same initial distribution and the same parameter set used in the comparison with data (see Table 1).

3.3.2 Sensitivity to initial conditions

For studying the sensitivity on initial conditions, the initial distribution has been changed by shifting the average diameter by $\pm 20\,\mu$m. Additionally, the initial distribution for the SCB model was calculated from the prescribed distribution function of the DB model. As can be seen in Figure 7 both models loose their dependence on the initial conditions after a short transient time and adapt their distributions to the hydrodynamical conditions after 2 h to 3 h. Hence, both models can be used in modeling situations with unknown initial conditions.
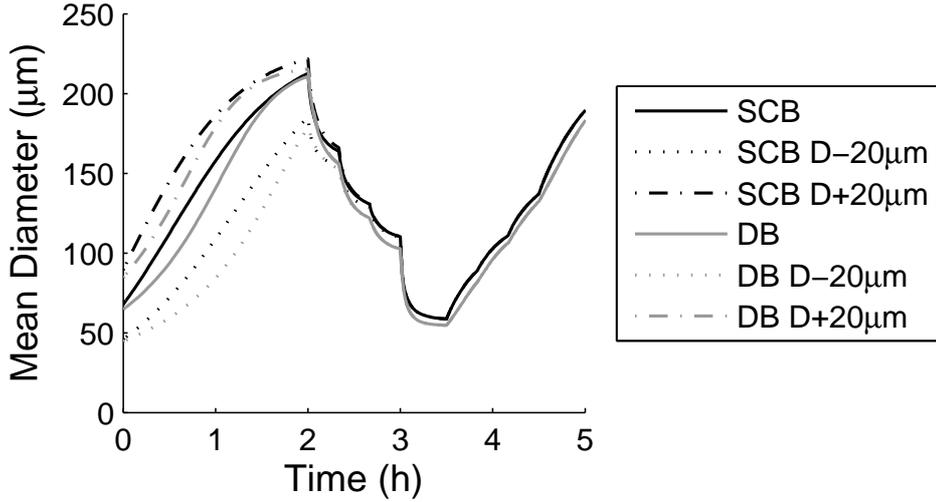
Fig. 7. Sensitivity of both models to initial conditions. SCB: size class-based model; DB: distribution-based model.

3.3.3 Sensitivity to fractal dimension

Since fractal dimension can be measured with various methods (e. g. Billiones et al., 1999; Manning and Dyer, 1999), often resulting in different values (from 1.5 to 2.4, Manning and Dyer, 1999), it is always a parameter of rather high uncertainty. Therefore its influence on model results must be examined. Our results reveal that a variation of d_f of about 5 % leads to a strong under- or overestimation of the average diameter for increasing or decreasing fractal dimension, respectively (cf. Figure 8). The SCB model is more sensitive to changes in fractal dimension than the DB model. As both aggregation and fragmentation rates are strongly dependent on the fractal dimension (directly and indirectly), it is the most sensitive parameter in both models. Furthermore, as can be seen from Eq. (21) and (22), fractal dimension strongly influences the vertical flux.

3.3.4 Sensitivity to collision efficiency, break-up factor and shear

The collision efficiency and the fragmentation factor are parameters that cannot be measured routinely, yet. These parameters are dependent on various influences like e. g. salinity (Van Leussen, 1994), organic matter content (Chen et al., 2005), involved phytoplankton species (e. g. Kiørboe et al., 1990), extracellular polymeric substances (EPS, e. g. Thornton, 2002; Dam and Drapeau, 1995), maybe the degradation state of aggregates as different settling velocities have been observed for differently degraded particles (Goutx et al., 2007), etc.

Moreover, collision efficiency and the break-up factor are closely related to
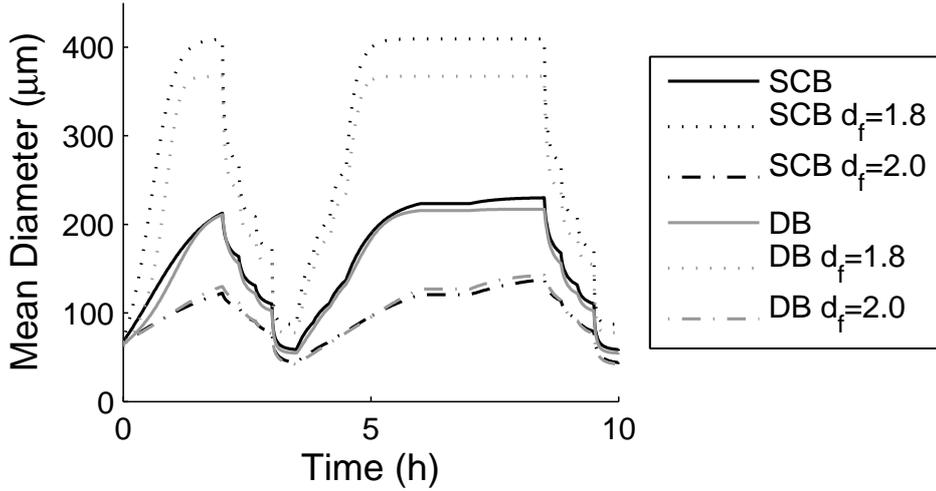
Fig. 8. Sensitivity of both models to changed fractal dimension compared to the reference runs. SCB: size class-based model; DB: distribution-based model.

each other. Furthermore, both processes, aggregation and fragmentation, always occur simultaneously. Together, they force the particle distribution to reach a steady state that is strongly dependent on the present hydrodynamic conditions. Hence, the influence of the collision efficiency and the break-up factor on the model behaviour should be examined together, but also in combination with the turbulent shear. Nevertheless, we first treat the parameters separately and study the influence of the collision efficiency on the model results by varying α by $\pm 5\%$. This corresponds to the same range of variation as for the fractal dimension. As can be seen by a comparison of Figure 8 and 9, both models are much less sensitive to changes of the collision efficiency than to fractal dimension. While the response of the mean diameter to a changed collision efficiency is linear, perturbations in d_f also lead to nonlinear effects that are even not uniform over time.

When examining both the collision efficiency and the break-up factor together, it is always possible to find a pair of these parameters to reach a defined steady state with both models, e. g. $\langle r \rangle^* = 100 \, \mu m$. This can be exemplarily seen in Figure 10A, that was calculated for the DB model. Obviously, the growth rates for a specific radius $\langle r \rangle$ are different for changed parameter pairs α and f_B. In model runs, this results in different curvatures of the time evolution. For different shear rates, the growth rates for a specific mean radius are also different, shown for the DB model in Figure 10B. Furthermore, the steady state shifts towards smaller radii for higher shear rates and vice versa. This effect is also nonlinear since different exponents are used for the dependence on shear in the aggregation and the fragmentation description. In principle, this behaviour, decribed for the DB model, can also be found for the SCB model.
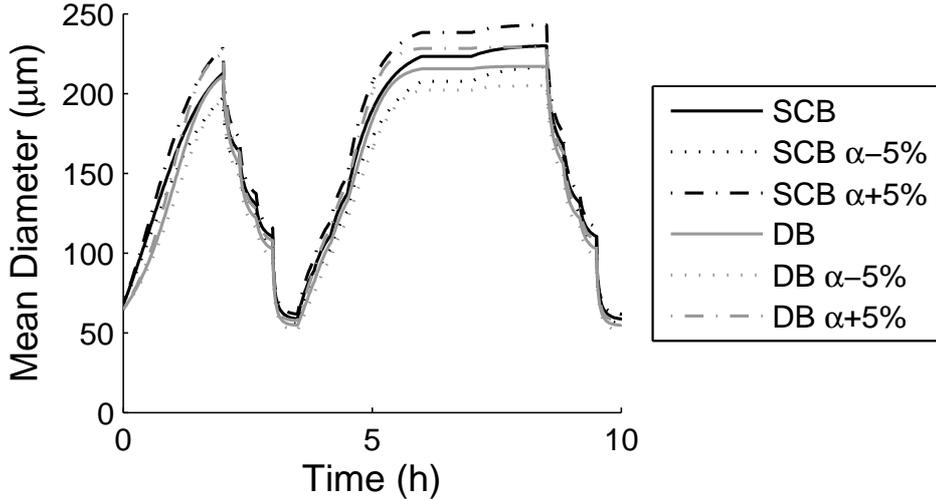
18

Fig. 9. Sensitivity of both models to variations in collision efficiency compared to the reference runs. SCB: size class-based model; DB: distribution-based model.

4 Discussion

In this study, two different kinds of flocculation models are compared. Their main difference is the representation of the particle distribution. While the SCB approach explicitly resolves a number of discrete size classes, the DB model uses variable moments of a prescribed distribution function.

In comparison to SPM size dynamics observed in a laboratory experiment, both models were able to reproduce the dynamics of the average diameter equally well, although both models exhibit a particle distribution smoother than the observed one that can either be caused by the numerical diffusion in the models (for the SCB model, see e.g. Prakash et al., 2003) or by the limited temporal resolution of the measurement probably loosing rare occuring large particles. On the other hand, a number of particles smaller than the resolution limit could have occured during the experiment. Moreover, floc restructuring may have occurred which would lead to changes of the fractal dimension (discussed e.g. by Verney et al., 2010, this issue). All the aforementioned reasons might limit the accuracy of the models' representation of the observed distribution (seen in Figure 4) and the goodness of the achieved $\alpha : f_{\mathrm{B}}$ couple. However, the sensitivity study showed a robust model behaviour in its dynamics concerning these two parameters, and hence, it is likely that both models could be useful to represent the floc dynamics disregarding a possible minor change in this parameter couple. Nevertheless, the models could be improved by i) better account for the numerical diffusion (SCB model) or other distributions (DB model, see below), and ii) introducing a variable fractal dimension.
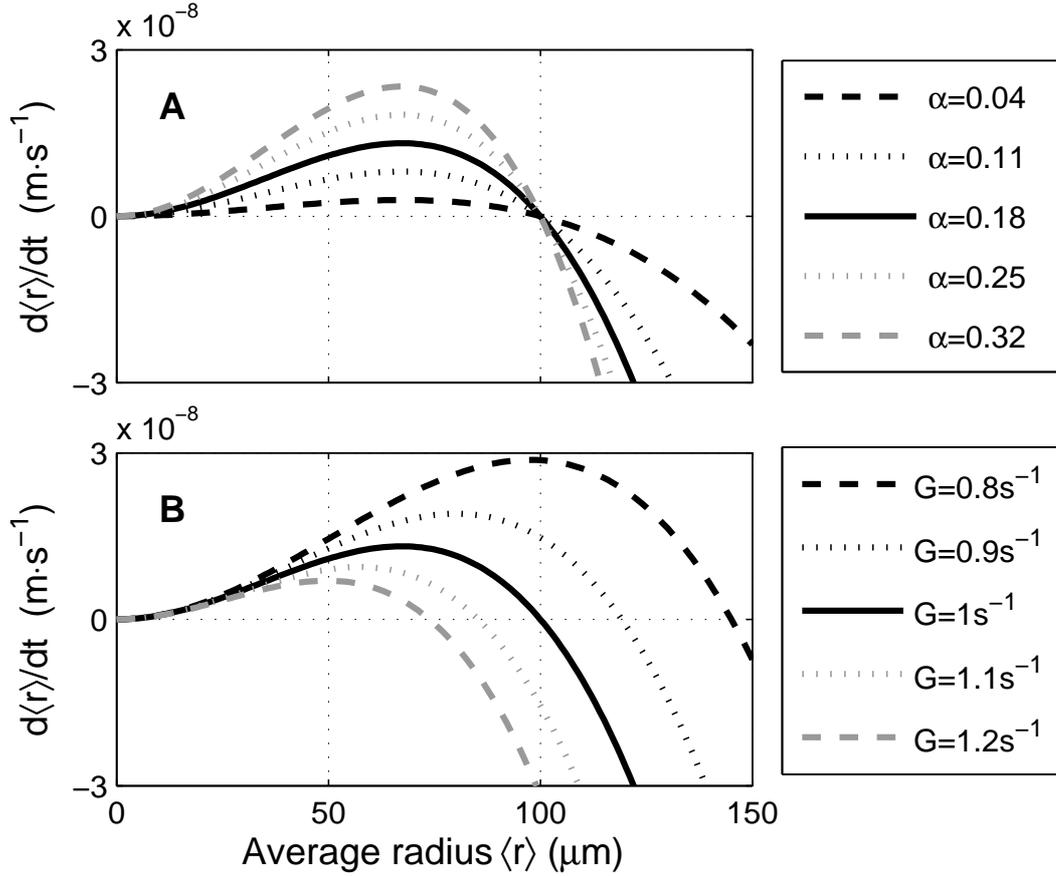
Fig. 10. Growth rates for the mean radius of the DB model. A) Different α and f_B pairs for the same steady state ($\langle r \rangle^* = 100\,\mu$m). The correspondent $\alpha{:}f_B$ values are: $0.04{:}2801\,\mathrm{s}^{1/2}{\cdot}\mathrm{m}^{-2}$, $0.11{:}7701\,\mathrm{s}^{0.5}{\cdot}\mathrm{m}^{-2}$, $0.18{:}12602\,\mathrm{s}^{0.5}{\cdot}\mathrm{m}^{-2}$, $0.25{:}17503\,\mathrm{s}^{0.5}{\cdot}\mathrm{m}^{-2}$, and $0.32{:}22404\,\mathrm{s}^{0.5}{\cdot}\mathrm{m}^{-2}$. B) The same α and f_B pair as for the reference run, but using different shear values.

Even in the sensitivity analysis, both models generally show the same behaviour. There are only slight differencies concerning the influence of the fractal dimension where the DB model is less sensitive than the SCB model. It turned out, that both models are most sensitive to changes of the fractal dimension as it contributes to aggregation and fragmentation in a nonlinear way. Fractal dimension is highly relevant for calculating the settling velocity and, hence, the vertical fluxes. In the presented laboratory experiment, the fractal dimension might be underestimated leading to uncertainties for the model runs. Its value, however, is in general difficult to obtain. Therefore, in order to improve and better validate flocculation models, we suggest to standardize measurements of fractal dimension or to aim for comparability of particles' fractal dimension values and to enhance knowledge related to changes of the fractal dimension. The latter is important to derive a process-based description for the change of the fractal dimension which could be included into – and improve – flocculation models.

Surface properties of flocs (like e.g. the cohesiveness), in the models represented by the collision efficiency α and the break-up factor f_B, have shown to be relevant for the reaction kinetics in terms of i) the reaction time, changing the curvatures in the time evolution and ii) the steady state. Therefore, supposing a qualitatively and quantitatively correct model formulation and known hydrodynamical conditions, it would be possible to access particles' surface properties by inverse modeling, as the strongly related parameter pair α and f_B could only be constrained in a small range. Inverse modeling studies had already been carried out for estimating the collision efficiency of organic aggregates by Kiørboe et al. (1990).

Structural differences in the model formulation and their underlying assumptions can explain the above mentioned discrepancies to observations and might limit the applications of both models. The SCB model would preferably be used to study the dynamical evolution of the shape of the particle distribution, like e.g. bimodal distributions (e.g. observed by Benson and French, 2007), since the type of distribution is preset in the DB model. Despite this fact, other features of the experimentally observed particle distribution, e.g. their mean settling velocity, can be well calculated by both models. Hence, the application of the DB model is not restricted to an exponential distribution but can also be used for similar distribution patterns. Intrinsically, the moment closure approach is independent of the functional form of the distribution and only gains accuracy for the Gaussian-like mass distribution assumed here. Therefore, it can also be used for other distribution functions. But this requires the reformulation of the model from first principles which can be a high analytical effort. Lacking flexibility is a deficit of the DB model compared to the SCB model. On the other hand, the DB model significantly reduces computational costs and hence, might be more suitable to be coupled to hydrodynamical models.

In the DB model, an implicit mass redistribution occurs during aggregation in such a way that the approximation of the prescribed distribution is fulfilled any time, as the growth rate for $\langle r \rangle$ is always based on this distribution function. This kind of mass redistribution is also present during fragmentation. By contrast, in the SCB model, the process of aggregation does not include an implicit fragmentation. Additionally, the SCB model faces the problem of numerical diffusion towards larger size classes due to logarithmically distributed size classes. These facts result in a smaller fragmentation factor f_B in the DB model although the collision efficiency had to be chosen smaller than in the SCB model. In general, one should keep in mind that different types of models require usually a different parametrization to describe the same experimental observations. These different parameters account for model-dependent internal realizations of the various processes even in cases where the basic assumptions about these processes are the same.

In comparison to empirical models of e. g. Manning and Dyer (1999, 2007) and Van Leussen (1994), process-based models like SCB and DB models are more flexible to use. Empirical models are more restricted since they are based on observations in a system with specific hydrodynamical, sedimentological and biological conditions. Nevertheless, as emphasized before, the DB model in its present form is also restricted to exponential-like particle number distributions. Therefore, the SCB model is the most flexible model, but with the drawback of high computational costs. Similar to the SCB model, the quadrature of moments method (QMOM; e. g. Prat and Ducoste, 2006) uses several weighting classes, but follows only the moments of the particle density function. This allows for higher flexibility compared to the DB model where the distribution function is prescribed. However, it is difficult to regenrate the size distribution by using the QMOM approach. Moreover, it has higher computational costs than the DB model.

In contrast to the model of Winterwerp (1998) the DB and the SCB model also provide information about the entire particle distribution. This is useful for calculating the mean settling velocity since it is not necessarily equal to the settling velocity of a particle having the average size (cf. Eq. (21) and (22)). Furthermore, other features, e. g. turbidity, can be obtained that are relevant in ecosystem models.

An application of the models in spatially explicit SPM transport models or ecosystem models has to face a number of remaining difficulties arising from model assumptions. Especially in case of the DB model, where a redistribution of mass, similar like during aggregation and fragmentation, will occur during transport. The same problem arises in the characteristic diameter based model when coupled to an 1 D vertical model (Winterwerp, 2002). Nevertheless, Kriest and Evans (2000) applied a DB aggregation model for the open ocean in a 1 D vertical model. In turn, due to different settling velocities of particles, numerical diffusion is different for each size class when applying the SCB model in an 1 D vertical model.

5 Conclusion

The size class-based (SCB) as well as the distribution-based (DB) model are able to represent the change of the average aggregate size, the floc distribution function and the mean settling velocity under different turbulent conditions. These findings indicate that both models have the potential to be included in spatially explicit models.

The fractal dimension is the most sensitive parameter in both models and can strongly influence the vertical flux. Therefore, it is necessary to enhance

the knowledge about processes that change the fractal dimension in order to improve SPM transport models.

At the present state, the application of the DB model is limited to exponential-like particle number distributions. Nevertheless, it is computationally very efficient. Furthermore, it can be applied to other distribution functions by reformulating the terms derived from the moment closure.

The main drawback of the SCB model is its high computational cost. On the other hand, it is more useful to represent temporally highly variable particle distribution patterns like bimodal distributions.

To conclude, the SCB model is useful to study the time evolution of floc distributions, especially under highly variable conditions. The DB model reduces the complexity of flocculation modeling. Hence, by a reduction of state variables, it is especially suitable to be coupled to spatially large scale SPM transport and biogeochemical models.

Acknowledgements

References

Benson, T., French, J. R., 2007. InSiPID: A new low-cost instrument for in situ particle size measurements in estuarine and coastal waters. Journal of Sea Research 58 (3), 167 – 188.

Billiones, R. G., Tackx, M. L., Daro, M. H., 1999. The geometric features, shape factors and fractal dimensions of suspended particulate matter in the Scheldt estuary (Belgium). Estuarine, Coastal and Shelf Science 48, 293 – 305.

Chen, M. S., Wartel, S., Temmerman, S., 2005. Seasonal variation of floc characteristics on tidal flats, the scheldt estuary. Hydrobiologia 540, 181 – 195.

Dam, H., Drapeau, D., 1995. Coagulation efficiency, organic-matter glues and the dynamics of particles during a phytoplankton bloom in a mesocosm study. Deep-Sea Research II 42 (1), 111 – 123.

Fettweis, M., 2008. Uncertainty of excess density and settling velocity of mud flocs derived from in situ measurements. Estuarine, Coastal and Shelf Science 78 (2), 426 – 436.

Goutx, M., Wakeham, S., Lee, C., Duflos, M., Guigue, C., Liu, Z., Moriceau, B., Sempere, R., Tedetti, M., Xue, J., 2007. Composition and degradation of marine particles with different settling velocities in the Northwestern Mediterranean sea. Limnology and Oceanography 39 (4), 1645 – 1664.

Guezennec, L., Lafite, R., Dupont, J.-P., Meyer, R., Boust, D., 1999. Hydrodynamics of suspended particulate matter in the tidal freshwater zone of a macrotidal estuary. Estuaries 22 (3), 717 – 727.

Kiørboe, T., Anderson, K., Dam, H., 1990. Coagulation efficiency and aggregate formation in marine phytoplankton. Marine Biology 107, 235 – 245.

Kranenburg, C., 1994. The fractal structure of cohesive sediment aggregates. Estuarine, Coastal and Shelf Science 39.

Kriest, I., Evans, G. T., 2000. A vertically resolved model for phytoplankton aggregation. Proc. Indian Acad. Sci. (Earth Planet Sci.) 109 (4), 453 – 469.

Krishnappan, B. G., 1991. Modelling of cohesive sediment transport. In: International Symposium on the transport of suspended sediments and its mathematical modelling. Florence, Italy, pp. 433 – 448.

Krishnappan, B. G., Marsalek, J., 2002. Transport characteristics of fine sediment from an on-stream stormwater management pond. Urban Water 4, 3 – 11.

Krone, R. B., 1962. Flume studies of the transport of sediment in estuarine shoaling processes. Tech. rep., University of California.

Lick, W., Huang, H., Jepsen, R., 1993. Flocculation of fine-grained sediments due to differential settling. Journal of Geophysical Research 98 (C6), 10279 – 10288.

Lunau, M., Lemke, A., Dellwig, O., Simon, M., 2006. Physical and biogeochemical controls of microaggregate dynamics in a tidally affected coastal ecosystem. Limnology and Oceanography 51 (2), 847–859.

Maerz, J., Wirtz, K. W., 2009. Resolving physically and biologically driven suspended particulate matter dynamics in a tidal basin with a distribution-based model. Estuarine, Coastal and Shelf Science 84 (1), 128 – 138.

Maggi, F., Mietta, F., Winterwerp, J., 2007. Effect of variable fractal dimension on the floc size distribution of suspended cohesive sediment. Journal of Hydrology 343 (1-2), 43 – 55.

Manning, A. J., Bass, S. J., Dyer, K. R., 2006. Floc properties in the turbidity maximum of a mesotidal estuary during neap and spring tidal conditions. Marine Geology 235, 193 – 211.

Manning, A. J., Dyer, K. R., 1999. A laboratory examination of floc characteristics with regard to turbulent shearing. Marine Geology 160, 147 – 170.

Manning, A. J., Dyer, K. R., 2007. Mass settling flux of fine sediments in Northern European estuaries: Measurements and predictions. Marine Geology, 107 – 122.

McAnally, W., Mehta, A. J., 2002. Significance of aggregation of fine sediment particles in their deposition. Estuarine, Coastal and Shelf Science 54, 643 – 653.

McCave, I. N., 1984. Size spectra and aggregation of suspended particles in the deep ocean. Deep-Sea Research 31 (4), 329 – 352.

Mikes, D., Verney, R., Lafite, R., Belorgey, M., 2004. Controlling factors in estuarine flocculation processes: experimental results with material from the Seine estuary, Northwestern France. Journal of Coastal Research SI 41, 82 – 89.

Prakash, A., Bapat, A. P., Zachariah, M. R., 2003. A simple numerical algorithm and software for solution of nucleation, surface growth, and coagulation problems. Aerosol Science and Technology 37, 892 – 898.

Prat, O. P., Ducoste, J. J., 2006. Modeling spatial distribution of floc size in turbulent processes using the quadrature method of moment and computational fluid dynamics. Chemical Engineering Science 61, 75 – 86.

Son, M., Hsu, T., 2008. Flocculation model of cohesive sediment using variable fractal dimension. Environmental Fluid Mechanics 10.1007/s10652-007-9050-7.

Thornton, D., 2002. Diatom aggregation in the sea: mechanisms and ecological implications. European Journal of Phycology 37, 149–161.

Van Leussen, W., 1994. Estuarine macroflocs and their role in fine-grained sediment transport. Phd thesis, University of Utrecht.

Verney, R., Brun Cottan, J. C., Lafite, R., J., D., Taylor, J. A., 2006. Tidally-induced shear stress variability above intertidal mudflats. case of the macrotidal seine estuary. Estuaries and Coasts 29 (4), 653–664.

Verney, R., Lafite, R., Brun-Cottan, J., 2010, this issue. Behaviour of a floc population during a tidal cycle: laboratory experiments and numerical modelling.

Verney, R., Lafite, R., Brun Cottan, J. C., 2009. Flocculation potential of natural estuarine particles: the importance of environmental factors and of the spatial and seasonal variability of suspended particulate matter. Estuaries and Coasts 32, 678 – 693.

von Smoluchowski, M., 1917. Versuch einer mathematischen Theorie der Koagulationskinetik kolloidaler Lösungen. Zeitschrift für physikalische Chemie 92 (2), 129 – 168.

Winterwerp, J. C., 1998. A simple model for turbulence induced flocculation of cohesive sediment. Journal of Hydraulic Research 36 (3), 309–326.

Winterwerp, J. C., 2002. On the flocculation and settling velocity of estuarine mud. Continental Shelf Research 22, 1339 – 1360.

Winterwerp, J. C., Manning, A. J., Martens, C., de Mulder, T., Vanlede, J., 2006. A heuristic formula for turbulence-induced flocculation of cohesive sediment. Estuarine Coastal and Shelf Science 68 (1-2), 195–207.

Wirtz, K., Eckhardt, B., 1996. Effective variables in ecosystem models with an application to phytoplankton succession. Ecological modelling 92, 33 – 53.

Xu, F., Wang, D.-P., Riemer, N., 2008. Modeling flocculation processes of fine-grained particles using a size-resolved method: Comparison with published laboratory experiments. Continental Shelf Research 28, 2668 – 2677.